COLD PLASMA TREATMENT OF MAGNETIC NANOPARTICLES

by

KE WANG

Presented to the Faculty of the Graduate School of

The University of Texas at Arlington in Partial Fulfillment

of the Requirements

for the Degree of

MASTER OF SCIENCE IN MATERIALS SCIENCE AND ENGINEERING

THE UNIVERSITY OF TEXAS AT ARLINGTON

August 2013

Acknowledgements

I would like to express my sincere gratitude to my research advisor, Professor J. Ping Liu, for guiding me into the scientific research field, and encouraging me to work in the field of cold plasma. The present research work would, therefore, have never been completed without his proper guidance, regular supervision, and constant encouragement. I would also like to express my deep gratitude to my research co-advisor Professor Richard B. Timmons for his encouragement, guidance and support throughout the course of this work. I have been fortunate to work with Dr. Timmons since he is a greatest scientist and mentor. He always gives me a lot of support, guidance and encouragement for the course of this work.

I particularly owe many thanks to Dr. Charles R. Savage for his sincere advice and assistance throughout my experiments. His technical support with equipments was a great help. Additionally, I wish to acknowledge Dr. Liu Xubo, Dr. Qiang Zhang and Dr. Kevin Elkins for their valuable assistance, collaboration and valuable discussions.

I would like to thank Professors Yaowu Hao and Jiechao Jiang for serving on my thesis supervisory committee. I am grateful to them for their careful and critical reading of my thesis and invaluable suggestions. Their comments and suggestions would not only help to improve my research skill but also would be a great help for my future research.

I would like to thank my colleagues, Dr. Narayan Poudyal, Dr.Vuong Van Nguyen, Dr.Yilong Ma, and Ms. Kinjal Gandha, for their cooperation in the laboratory activities. There can be no enough acknowledgements for the loving encouragement I have received from my parents, without their constant support and inspirations all this would never have been possible.

May 08, 2013

Abstract

COLD PLASMA TREATMENT OF MAGNETIC NANOPARTICLES

Ke Wang, M.S.

The University of Texas at Arlington, 2013

Supervising Professor: J. Ping Liu and Richard B. Timmons

This thesis investigates the application of cold plasma to remove the oleic acid bonded on magnetic nanoparticles: $SmCo_5$ nanoflakes prepared via surfactant assisted high energy ball milling and $CoFe_2O_4$ nanoparticles prepared via chemical synthesis. Oleic acid molecules bonded on nanoparticles are in the carboxylate form which could not be washed away by organic solvents in ultrasonic bath; only free oleic acid molecules left on the nanoparticle surface after ball milling can be washed away through ultrasonic bath. High temperature annealing method works for removing oleic acid but nanoparticles would be damaged because of oxidation and decomposition.

The RF cold plasma has advantages over above methods as the plasma temperature is typically around room temperature, and the energetic ions could strike away carboxylate molecules bonded on the surface of nanoparticles without changing the surface chemistry. Powder X-ray diffraction (XRD) was performed to see if there was phase transformation, decomposition during plasma treatment. The content change of oleic acid moleculs on the nanoparticles surface was confirmed by X-ray photoelectron spectroscopy (XPS) and Fourier transform infrared spectroscopy (FTIR).

Table of Contents

Acknowledgements iii

Abstract iv

List of Illustrations vii

List of Tables ixx

Chapter 1 Introduction 1

1.1 Fundamentals of Magnetic Materials 1

1.1.1 Introduction of Magnetic Materials 1

1.1.2 Classification of Ferromagnetic Materials for Applications 2

1.2 Surfactant Use in Magnetic Nanoparticle Sythesis 5

1.3 Introduction to Plasma Treatment 7

1.4 Motivations for Applying Argon Cold Plasma on Cleaning Surfactants 10

Chapter 2 Experimental 12

2.1 Magnetic Nanoparticle Synthesis 12

2.1.1 Experimental Procedure for Synthesis of $CoFe_2O_4$ Nanoparticles 12

2.1.1.1 Synthesis of 4 nm $CoFe_2O_4$ nanoparticles 12

2.1.1.2 Synthesis of large (> 6 nm) $CoFe_2O_4$ nanoparticles 14

2.1.2 Surfactant-assisted Ball-milling of $SmCo_5$ Nanoparticles 14

2.2 Cold Plasma Cleaning Process 15

2.2.1 Introduction of Cold Plasma and Motivation of Cold Plasma Cleaning 15

2.2.2 Principles of Argon Cold Plasma Cleaning 18

2.2.3 Experimental Set-up for Cold Plasma Treatment 19

2.2.4 Experimental Details for Cold Plasma Cleaning 23

2.2.4.1 $CoFe_2O_4$ nanoparticles 23

2.2.4.2 $SmCo_5$ nanoflakes 23
2.3 Characterization of Plasma Treated Magnetic Nanoparticles 24
2.3.1 XPS and FTIR 24
2.3.2 X-ray Diffraction (XRD) 25
Chapter 3 Results and Discussion 26
3.1 Experiments of Cleaning Surfactant on $CoFe_2O_4$ Nanoparticles 26
3.2 Experiments of Plasma Cleaning Surfactants on $SmCo_5$ Nanoflakes 28
3.2.1 Experiments to Confirm the Effect of Plasma Cleaning 28
3.2.2 Effect of Pressure on Plasma Cleaning 37
3.2.3 Effect of Treating Time on Plasma Cleaning 38
Chapter 4 Summary 41
References 44
Biographical Information 47

List of Illustrations

Figure 1-1 The orbit of a spinning electron about the nucleus of an atom 2

Figure 1-2 *M-H* curves for soft and hard magnets 3

Figure 1-3 Progress in the energy product of permanent magnets in the 20^{th} century 5

Figure 1-4 Boiling point with respect to surfactant molecular weight for the free (unbound) molecule 6

Figure 2-1 Scheme for synthesis of $CoFe_2O_4$ nanoparticles 12

Figure 2-2 Heating profile for synthesis of (A) 4 nm and (B) 6 nm $CoFe_2O_4$ nanoparticles 13

Figure 2-3 Diagram of a carboxylate Ion (Left), R is an organic group, and a free oleic acid molecule (Right) 18

Figure 2-4 Schematic diagram of the rotary plasma reactor system employed for the nanoparticles surface cleaning 20

Figure 2-5 Picture of the rotary plasma reactor with elecreodes outside of glass reactor 21

Figure 2-6 Newly designed glass reactor for plasma treatment of SmCo powders..... 22

Figure 2-7 Picture of the glass reactor under plasma treatment 22

Figure 3-1 FTIR (ATR) results of oleic acid on cobalt ferrite nanoparticles before (Blue) and after (Red) plasma treatment 26

Figure 3-2 FTIR(Transmission) results of oleic acid on cobalt ferrite nanoparticles before(Red) and after(Blue) plasma treatment 26

Figure 3-3 XPS results of surface composition on cobalt ferrite nanoparticles before plasma treatment 27

Figure 3-4 XPS results of surface composition on cobalt ferrite nanoparticles after plasma treatment 28

Figure 3-5 XPS results of surface compositon on $SmCo_5$ nanoflakes before plasma treatment 30
Figure 3-6 XPS results of surface compositon on $SmCo_5$ nanoflakes after plasma treatment for 180 minutes 31
Figure 3-7 TGA results of ball-milled $SmCo_5$ nanoparticles before and after plasma treatment (30min) 32
Figure 3-8 X-ray diffraction patterns of untreated and plasma-treated (180min) ball-milled $SmCo_5$ nanoflakes 33
Figure 3-9 FTIR (ATR mode) results of OA on untreated ball-milled $SmCo_5$ nanoflakes and untreated $SmCo_5$ nanoflakes with free oleic acid 34
Figure 3-10 FTIR (ATR mode) results of OA on untreated ball-milled $SmCo_5$ nanoflakes and Cobalt Ferrite nanoparticles 35
Figure 3-11 FTIR (Transmission mode) results of untreated ball-milled $SmCo_5$ nanoflakes (Four times of measurement for the same sample) 36
Figure 3-12 X-ray diffraction patterns of untreated and plasma-treated (under different pressure) $SmCo_5$ nanoflakes 37
Figure 3-13 At % change of C 1s, Sm $3d_{5/2}$, Co $2p_{3/2}$ and Sm $3d_{5/2}$+Co $2p_{3/2}$ with different treating pressure 38
Figure 3-14 X-ray diffraction patterns of untreated and plasma-treated (under different treating time) $SmCo_5$ nanoflakes 39
Figure 3-15 At % change of C 1s, Sm $3d_{5/2}$, and Co $2p_{3/2}$ with different treating time 40

List of Tables

Table 2-1 Internal and External Parameters in a Plasma System 17

Table 2-2 The Parameters for Plasma Treatment of the Samples under Different Pressure 23

Table 2-3 The Parameters for Plasma Treatment of the Samples under Different Treating Time 24

Table 3-1 Atomic Percentage (At %) Change with Different Treating Time on $SmCo_5$ Nanoflakes from XPS Results 29

Table 3-2 At% Ratio Change of C1s/Sm $3d_{5/2}$, and C1s/(Sm $3d_{5/2}$ + Co $2p_{3/2}$) with Treating Time on $SmCo_5$ Nanoflakes from XPS Results 29

Chapter 1

Introduction

1.1 Fundamentals of Magnetic Materials

1.1.1 Introduction of Magnetic Materials

The phenomenon that magnetic materials can exert an attractive or repulsive force to other magnetic materials is what we called magnetism. All the magnetic materials are influenced by the presence of magnetic field to some degree, even though in most cases such influence is so small that can only be detected by certain equipments. Whenever electrically charged particles are in motion, magnetic field is yield. This can arise either from the movement of electrons in an electric field, resulting in "electromagnetism", or from the constant subatomic movement of electrons, resulting in what is known as "permanent magnetism" [1-3].

There are two kinds of electronic motion in the matter if we view from atomic level: the orbital motion and the spin motion. These two types of electronic motions are the major sources of the macroscopic magnetic phenomena in materials. There are also some nucleic magnetic effects, which are much smaller when compared with the above two. Each electron may also be thought of self-spinning around its own axis, which yields a spin moment. Another magnetic moment comes from the electronic motion along the orbit around the atomic nucleus, as shown in Figure 1-1. The net magnetic moment of an atom is the sum of the magnetic moments of each of the constituent electrons, both orbital and spin contributions are included. Moment cancellations due to opposite direction of electrons moment paired are also needed to be taken into account [2-6]. If materials are composed of atoms have completely filled electron shells in, they are not capable of being permanently magnetized.

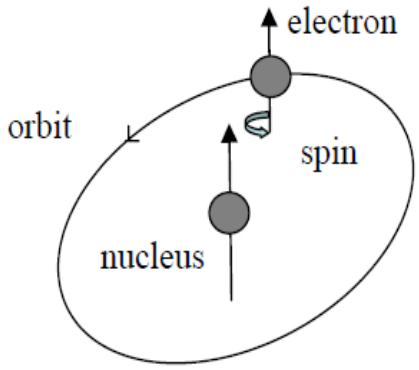

Figure 1-1 The orbit of a spinning electron about the nucleus of an atom

The types of magnetism are classified as diamagnetism, paramagnetism, and ferromagnetism; antiferromagnetism and ferrimagnetism are subdivisions of ferromagnetism [4].All materials have the property of at least one of above types of magnetism.

1.1.2 Classification of Ferromagnetic Materials for Applications

Magnetic materials can be classified into soft and hard magnetic materials group according to their hysteresis characteristics [2-6].

Soft Magnetic Materials and Their Applications [2-6]: Soft magnetic materials can be magnetized and demagnetized easily through the application of low strength magnetic field. A state of low residual magnetization is returned for this type of magnetic materials after the magnetic field is removed. Soft magnetic materials are used primarily to enhance or channel the flux produced by an electric current. The relative permeability is an important parameter, and it measures how readily the material responds to the applied magnetic field. As for Soft magnetic materials, typically their intrinsic coercivity is less than 100Oe, and with a high saturation magnetization but low coercivity, as shown in Figure 1-2. The application for soft magnetic materials fall into two groups: DC and AC.

As far as the DC application, the magnets is magnetized first and then demagnetized to complete a whole operation, for example: by switching on an electromagnet on a crane at a scrap yard will attract a scrap steel and drop it by switching off. For AC applications, the magnets are continuously cycled being magnetized in one direction to the other in the operation, such as a power supply transformer.

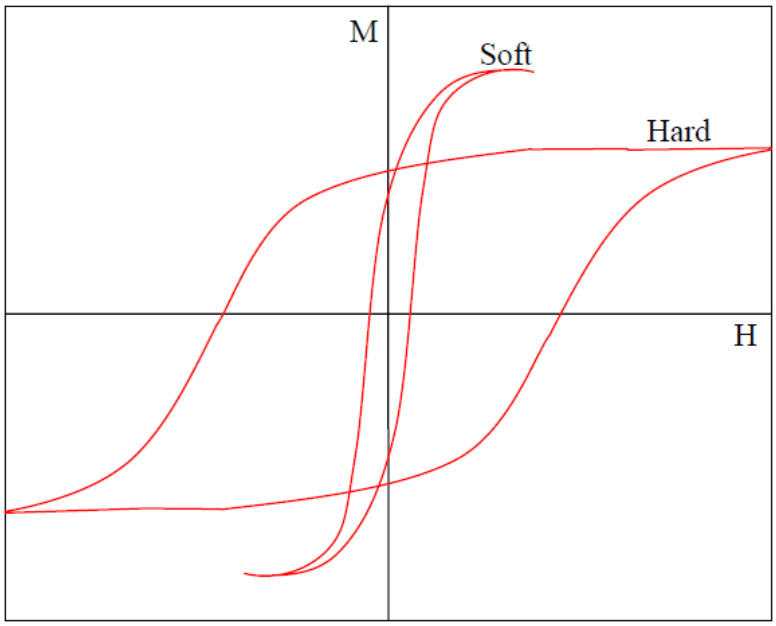

Figure 1-2 *M-H* curves for soft and hard magnets

Hard Magnetic Materials and Their Applications: Hard magnets are also called permanent magnets, in which their magnetism can be retained after being magnetized. “Hard” referred to as having sufficiently high resistance to demagnetizing field. Coercivity is used to distinguish between hard and soft phase magnetic materials, as shown in Figure 1-2. Hard materials have an intrinsic coercivity larger than 1000Oe and typically have high remanence *Mr*, therefore their energy product *(BH)max* is high.

Some of the applications of hard magnetic materials are as follows [7]:

Automotive: Starter motors, anti-lock braking systems (abs), motor drives for wipers, injection pumps, fans and controls for windows, seats etc, loudspeakers, eddy current brakes, alternators.

Telecommunications: Loudspeakers, microphones, telephone ringers, electro-acoustic pick-ups, switches and relays.

Data Processing*:* Disc drives and actuators, stepping motors, printers.

Consumer Electronics: DC motors for showers, washing machines, drills, low voltage dc drives for cordless appliances, loudspeakers for TV and audio, TV beam correction and focusing device, compact-disc drives, home computers, video recorders, clocks. Electronic and Instrumentation: Sensors, contactless switches, NMR spectrometer, energy meter disc, electro-mechanical transducers, crossed field tubes, flux-transfer trip device, dampers.

Industrial: DC motors for magnetic tools, robotics, magnetic separators for extracting metals and ores, magnetic bearings, servo-motor drives, lifting apparatus, brakes and clutches, meters and measuring equipment.

Astro and Aerospace: Frictionless bearings, stepping motors, couplings, instrumentation, travelling wave tubes, auto-compass.

Biosurgical: Dentures, orthodontics, orthopedics, wound closures, stomach seals, repulsion collars, ferromagnetic probes, cancer cell separators, magnetomotive artificial hearts, NMR / MRI body scanner.

There are some other types of alloys, intermetallics and ceramics of hard magnetic materials are being intensively studied, eg, Cobalt-rare earth alloys ($SmCo_5$, or Sm_2Co_{17}), neodymium-iron-boron ($Nd_2Fe_{14}B$), iron-platinum (FePt), cobalt-platinum (CoPt), hard ferrites ($SrO\text{-}Fe_2O_3$ or $BaO\text{-}6Fe_2O_3$), and Alnicos.

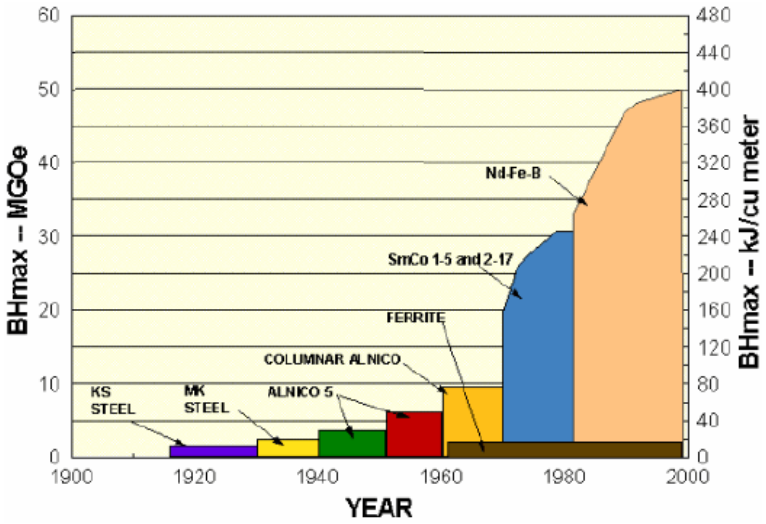

Figure 1-3 Progress in the energy product of permanent magnets in the 20th century

The coercivity and the maximum energy product have been enhanced a lot for rare-earth-transition-metal permanent magnets during the past century. Figure 1-3 shows the energy products development of those hard magnetic materials.

1.2 Surfactants Use in Magnetic Nanoparticles Synthesis

Surfactant-assisted ball milling is an important technique in producing micron or nanometer size particles with nano-scale feature in materials research and application. This technique has been used to obtain rare-earth magnetic nanoparticles and nanostructured powders. The functional moiety in surfactants molecules can physically, chemically or electrically react with the metal particles' surface during the process of deformation and new surfaces are exposed, which makes the surfactant as a key factor in ball milling. The surfactant molecules attached on the new surface to form a thin organic layer to protect the surface from cold welding when the new surface get contact with another surface during the ball-milling process. By changing the ratio between powder and surfactants, different varieties of structures, morphologies, and feature of the final product can be obtained. [8-9]

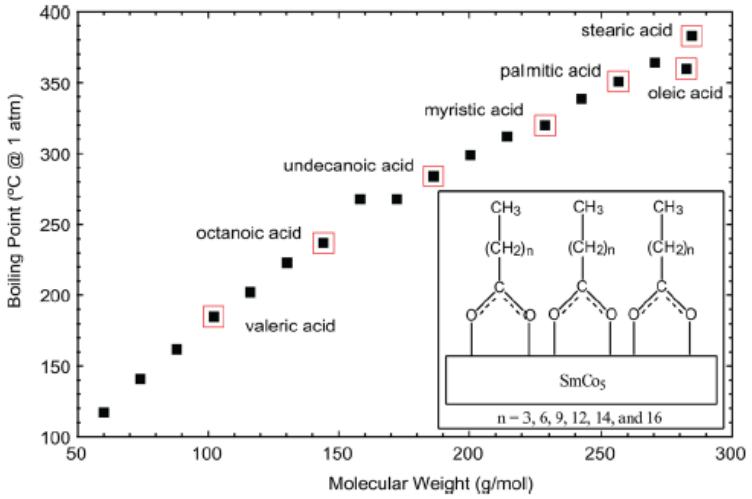

Figure 1-4 Boiling point with respect to surfactant molecular weight for the free (unbound) molecule. (Inset: Illustration of the carboxylate bonding of a fatty acid to $SmCo_5$ surface resulting in the formation of an organic film.) [8]

Surfactant assisted high energy ball milling has recently been utilized in making nanostructrued $SmCo_5$ powders with diameters less than 30 nm and with different morphologies ranging from flaks to spherical particles. Surfactant played a key role in the ball milling process but it often need to be removed after the ball milling before the consolidation of powders. Otherwise, due to the high pressure or temperature required in the process of consolidation, the surfactants may decomposed and react with the metal surface to yield impurities in the final products. Surfactant can be removed through vacuum annealing, high temperature and long dwell time is need for this process, but this will result in grain growth and oxidation for the magnetic nanostructured powders. From the literature report, mostly oleic acid (OA) is used as surfactant to prepare $SmCo_5$ nanoflakes. Oleic acid interacts with $SmCo_5$ in the process of ball milling and a carboxylate bond formed between the metal surface and the carboxylate acid head of the surfactant, Figure 1-4. Typically 500 ºC or higher temperature is required to remove the

OA attached on the metal surface, because of the chemical reaction. [8] It is also known that for the $SmCo_5$ powders after ball milling, there is still a large amount of oleic acid bonded on the metal surface even after repeated (8 times) washing in an ultrasonic bath with haptane and ethanol, and the remaining OA on the metal surface is the cause of oxidation of $SmCo_5$ nanoflakes surfaces or interfaces in the process of hot pressing. [10]

1.3 Introduction to Plasma Treatment [11-12]

Plasma is the fourth state of the matter, when taken into consideration of the energy of the particles constituting it, compared with solid, liquid, and gas. Langmuir first time used the term “plasma” in 1929 to describe ionized gases. Since the plasma was first discovered, a lot of efforts have been done to better understand the plasma state and most importantly to take advantage of it as a processing technology tool. Since 1960’s plasma process has been developed in the microelectronics industry and this is the first drive force for plasma research and technology. We can see the plasma technology application in many other fields nowadays such as biomedical, automotive, textile, lightening and many others applications that deal with surface modification [13].

When sufficient energy higher than the ionization energy is applied to the gas, plasma can be obtained. This caused ionization and production of ions and electrons. Parallel and concomitant to this ionization is the recombination of electrons with ions to form neutral particles. In a gas the plasma is excited and sustained by electromagnetic energy adding to the gas in many forms: direct current, radio frequency, microwaves and etc. The most common way to produce plasma is by providing an electrical discharge on the gas and this is the reason why plasma can be referred to as gas discharge.

Plasmas can be classified into several categories: First is plasma in complete thermodynamic equilibrium. In this plasma all temperatures such as the temperature of gas and electron temperature of the plasma are equal and it exists only in stars or during

the short interval of a strong explosion. No practical importance for this plasmas because they do not exist in controlled laboratory conditions. Second is plasma in local thermodynamic equilibrium. All temperatures except the radiation temperature are equal in each small volume of this plasma. The third is plasmas that are not in any local thermodynamic equilibrium. These plasmas are also name as cold plasma. Plasmas in local thermodynamic equilibrium and plasmas not in any local thermodynamic equilibrium are produced for research or manufacturing purposes, designated as thermal and cold plasma respectively.

Plasmas in local thermodynamic equilibrium can exist in two conditions: when the heavy particles are very energetic, at temperatures of the order of 10^6-10^8 K, and the other is at atmospheric pressure, even at temperatures as low as 6000 K. In low pressure discharge thermodynamic equilibrium cannot be reached, even between the electrons and the heavy particles at a local scale. This type of plasma is the plasmas that are not in any local thermodynamic equilibrium, and in this plasma the temperature of electrons is much higher than that of the heavy particles. The temperature of electrons can reach temperatures as high as 10^4-10^5 K, while the temperature is low as room temperature for the gas, and this type of plasma is called cold plasma. This is because there is no heat exchange between large particles(when compared with electrons) such as ions, atoms and molecules and electrons, and electrons move much faster than the other large particles, those spices(large particles) are kept almost at room temperature. Therefore this type of plasma present room temperate or some maybe slightly higher than room temperature but should be less than 100ºC in general.

Low pressure and generation of an electrical field are needed in order to activate and sustain this type of plasma, or namely cold plasma. The number of free electrons tremendously increases once the electrical field is applied to the system. Electrons are

accelerated and collide with large particles to produce excited species, molecular fragment and new electrons. Pressure must be low, because more collisions will happen between elections and ions as pressure increases, and if the pressure is high enough ions and excited species cannot be formed or the life time is too short to sustain stable plasma. Therefore in steady state plasma the process of ionized and excited spices production and the recombination of those activated species happen at the same time and are balanced. Natural plasma can be generated during Aurora Borealis or Northern Lights. Because of the gas-like state plasma can treat materials with special shapes and complex geometries such as webs, tubes and powders [14-16]. Plasma has advantages over other processes because of its super reactivity and unique chemistry and this can obtain final surface properties could cannot reached by other treatments. Furthermore no solvents are needed and very few amount of chemical used at some certain treatment this make plasma as environmentally friendly. There types are used a lot during the past decades:

1) Etching or ablation: Surface of substrate can be removed by energetic positive ions in plasma. It can be used as a surface cleaning tool or to obtain specific patterning [17].
2) Plasma deposition: It is also called Plasma Enhanced Chemical Deposition (PECD). Reactive species in the plasma can be chemically reacted between themselves and form thin films on the surface of substrate [18].
3) Plasma functionalization: Plasma species react with the substrate surface in certain spots, they do not react among themselves. New functional groups will be attached on the surface of the substrate [19].

Properties such as adhesion, biocompatibility, hardness, wettabbility and etc can be modified by plasma treatments. Compared with small size particles, flat surfaces, even foils and webs are much easier treated by using cold plasma [14, 20]. More difficult

process, equipment or system complexity and difficulty in treatment homogeneity make powders plasma treatment difficult and this is the reason why not so much research has been worked on powder materials. In this thesis powders materials treatment will be focused only as we only works on this type of materials.

1.4 Motivations for Applying Argon Cold Plasma on Cleaning Surfactants

Ball milling is an effective technique to produce rare-earth containing nanoparticles and is a new way in industry for the fabrication of nanostructured magnetic materials. [8] For conventional ball milling (wet or dry) of metal materials, even an extended milling time is applied, the average particles size is submicron meter minimum. This is because of fine particles cold welding again in the process. Improvements can be made by adding surfactants along with organic solvents in wet ball milling. For surfactant assisted ball milling, milling efficiency and particles size reduction can be reached as surfactants can prevent cold welding in ball milling, and down to nanoscales size of the particles can be obtained. [9] In the 1990s, Cambell *et al* [21] and Kaczmarek *et al* [22] used surfactants during wet milling of barium ferrite and observed a rapid decrease in powder particles size and homogenization with milling time. In 1996, Kirkpatrick *et al* [23] reported that particles size obtained by ball milling of the SmCo powder with surfactant was smaller than those milled without surfactant. Oleic acid is mainly used as the surfactants in the ball milling of Sm-Co and Nd-Fe-B nanoparticles. It is known that for the ball milled $SmCo_5$ nanoparticles, there is large amount of surfactants remaining on the particles surface even after repeated washing in an ultrasonic bath with different solvents such as haptane and ethonal. [10] This is because oleic acid interacts with the metal particles surface to form carboxylate bond between the carboxylate acid head of the surfactant and the metallic surface of $SmCo_5$. [8] In the ball milling process, results show that surfactants are harmful to magnetic nanoparticles in the processing of high-

temperature compaction. [9] This is because the surfactants remaining on the surface of nanoparticles will lead to oxidation of $SmCo_5$ at the surface/interface of nanoparticles and decomposition to Sm_2Co_{17} during hot-pressing process. [10] Oleic acid has a bolling point of 360ºC and this makes it brings an issue of complete removal of the surfactants after ball milling. Besides, nanostructured materials exposed to high temperature for removal of surfactant will result in grain growth and oxidation. [8] In order to preserve the nanoscale features it would be desirable to try other techniques for the surfactant removal. Low pressure inert gas plasma is very promising in removing the organic surfactant surface because of the high energetic ions etching. The temperature is relatively low (room temperature), and the surface of the metallic will not be chemically altered as this etching process is a physical method. The Argon cold plasma can remove organic contaminants on the surface of metals and the rotary cold plasma system works with nanoparticles plasma treatment [24-28, 34]

Chapter 2

Experimental

2.1 Magnetic Nanoparticle Synthesis

2.1.1 Experimental Procedure for Synthesis of $CoFe_2O_4$ Nanoparticles

The synthesis was done through a standard airless process [1]: The reagents were obtained from commercial sources and used without further treatment. Co-ferrite ($CoFe_2O_4$) nanoparticles were synthesized by simultaneous chemical reduction of iron (III) acetylacetonate $Fe(acac)_3$, and cobalt (II) acetylacetonate $Co(acac)_2$, by 1,2-hexadecanediol at high temperature in solution phase. Particle diameter was tuned from 3 nm to 20 nm by varying reaction conditions or by seed-mediated growth method.

2.1.1.1 Synthesis of 4 nm $CoFe_2O_4$ nanoparticles

As for 4 nm particles, the composition was controlled by varying the mole ratios of the precursors $Fe(acac)_3$ and $Co(acac)_2$ used during the chemical synthesis [1]. $Fe(acac)_3$ (1 to 3 mmol), $Co(acac)_2$ (1 mmol), 1,2-hexadecanediol (10 mmol), oleic acid (5 mmol), oleylamine (5 mmol), and phenyl ether (20 ml) were mixed and magnetically stirred under a flow of Ar for 30 minutes.

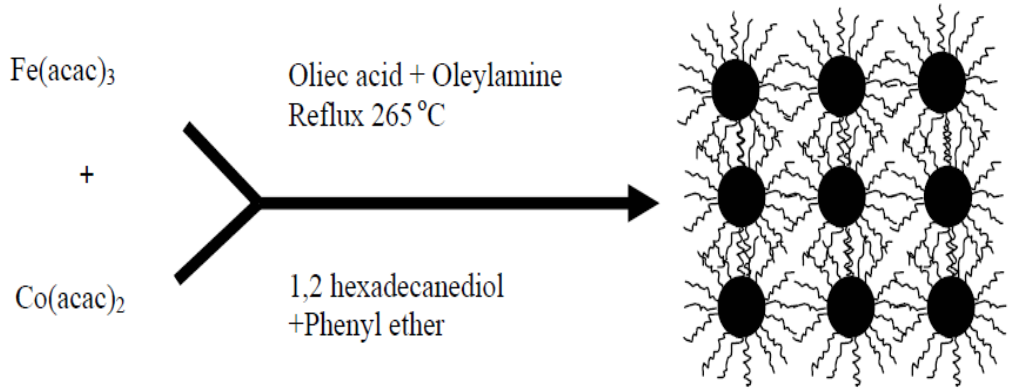

Figure 2-1 Scheme for synthesis of $CoFe_2O_4$ nanoparticles [1]

The flask was then heated to 100 °C and held for 20 min. During this hold, 5 mmol (1.7 ml) of oleylamine and 5 mmol (1.6 ml) of oleic acid were injected into the flask while continuing the Ar purge. After the 20 min hold, the mixture was maintained under an Ar blanket and heated to 200 °C and held for 20 minutes and then heated to 265 °C at a rate of approximately 10 °C per minute. The flask was maintained at the refluxing temperature of 265 °C for 30 min before it was cooled down to room temperature under the Ar blanket. The heating profile used for this process is shown in Fig 2-2 (A).

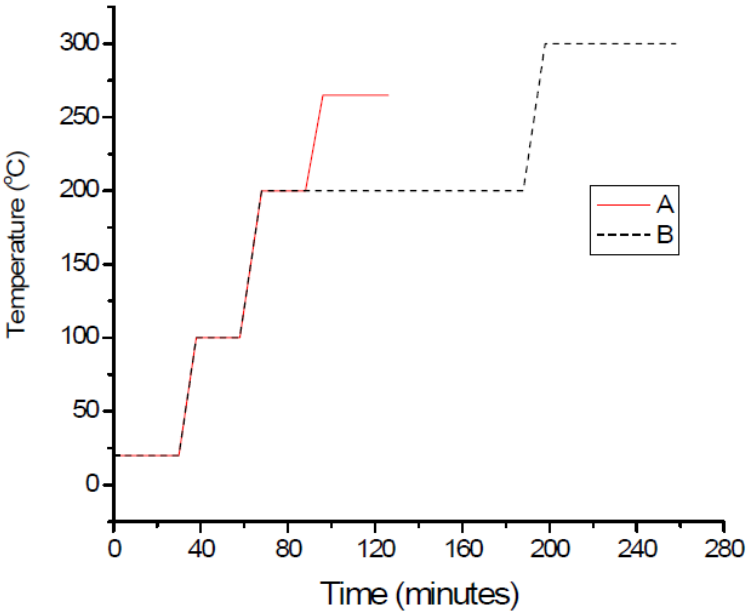

Figure 2-2 Heating profile for synthesis of (A)4 nm and (B)6 nm $CoFe_2O_4$ nanoparticles [1]

Purification of the nanoparticles was accomplished as follows: 5 ml of the dispersion taken from the flask was added to 20 ml of ethyl alcohol (ethanol) and the mixture was centrifuged at 6000 rpm for 15 min. The supernatant was discarded and the precipitate redispersed in 10 ml of hexane and 5 ml of ethanol. Additional small amount of oleylamine and oleic acid is added to aid in redispersing the nanoparticles. This dispersion was centrifuged at 6000 rpm for 15 min. The supernatant was transferred to a new centrifuge tube, and any precipitate was discarded. An additional 15 ml of ethanol

was added to this dispersion and centrifuged again. The supernatant was discarded and the remaining dark brown precipitate was re-dispersed in hexane to form 4 nm $CoFe_2O_4$ nanoparticles. 6 nm particles were prepared by replacing phenyl ether with benzyl ether and following the profile (see Figure 2-2(B)).

2.1.1.2 Synthesis of large (> 6 nm) $CoFe_2O_4$ nanoparticle

Molar ratios of 1.5:1 of $Fe(acac)_3$ and $Co(acac)_2$ was kept constant to prepare bigger particles. Particles of bigger size were prepared by seed-mediated growth method using the 4 nm and 6 nm as seeds. In this process, the smaller $CoFe_2O_4$ nanoparticles (as seeds) were mixed with more precursor materials and the mixture was heated as in the synthesis of 4 nm or 6 nm particles. By controlling the quantity of nanoparticle seed, $CoFe_2O_4$ nanoparticles with various sizes can be synthesized. For example, mixing and heating 60 mg 4 nm $CoFe_2O_4$ particles with 1.5 mmol of $Fe(acac)_3$, 1 mmol of $Co(acac)_2$, 8 mmol of 1, 2-hexadecanediol, 2 mmol of oleic acid, and 2 mmol of oleylamine formed 8 nm $CoFe_2O_4$ particles. Similarly, mixing and heating 50 mg of 8 nm $CoFe_2O_4$ seed particles with 2 mmol of $Fe(acac)_3$, $Co(acac)_2$, 8 mmol of 1,2-hexadecanediol, 2 mmol of oleic acid, and 2 mmol of oleylamine formed 12 nm $CoFe_2O_4$ particles , while changing to mass of seeds into 20 and 15 mg formed 15 and 20 nm $CoFe_2O_4$ nanoparticles respectively.

2.1.2 Surfactant-assisted Ball Milling of $SmCo_5$ Nanoparticle

The surfactant-assisted ball milling technique has been used to prepare magnetic nanopaticles. [29] The raw materials, commercially available $SmCo_5$ powders, have particle sizes from ~10 to 45 μm. The organic solvent heptane (99.8% purity) was used as the milling medium and oleic acid (90%) were used as the surfactants during milling. The powders were ground in a milling vial with balls made of 440C hardened steel by using a Spex 8000M high-energy ball milling machine. The milling process and handling

of the starting materials and the milled products were carried out in an argon gas environment inside a glove box to protect the particles from oxidation. In this experiment, the typical milling duration used was 120 min with balls of 1/4 inch in diameter. The weight ratio of powder to ball was set as 1:10. The amount of surfactant used was ~50% and the solvent used was about 55% of the weight of the starting powder, respectively. The ground slurry was then transferred to a 50 ml centrifugal tube, dispersed into heptane and ethanol solvent by ultrasonic vibration, and washed through centrifugal. This physical way of cleaning cannot remove the oleic acid that is bonded on the ball-milled magnetic nanoparticles.

The surfactants used in ball milling are absorbed by the fresh surface of particles crushed during the ball milling, leading to a surface modification for the ground particles. Experimental results show that the function of the surfactants is multifold: (1) The surfactants prevent the re-welding of the crushed particles during the ball milling; thus fine particle size can be obtained. (2) The surfactant-induced surface modification can greatly enhance the dispersion of $SmCo_5$ nanoparticles in a solvent. (3) The oil-like surfactants coated on the surfaces also act as lubricants on the particle surfaces, which reduces contamination.

2.2 Cold Plasma Cleaning Process

2.2.1 Introduction of Cold Plasma and Motivation of Cold Plasma Cleaning [11-12, 30-31]

Plasma are quasi-neutral particles systems in the form of gaseous mixtures of electrons, free radicals, ions, photons and a great number of neutral molecules in both ground and excited states. When sufficient energy which is higher than the ionization energy is added to atoms of a gas, causing ionization and production of electrons, plasma is obtained. Recombination of electrons with ions to form neutral atoms or molecules occurs parallel and concomitant to the ionization. Plasma is excited and

sustained by providing electromagnetic energy: direct current, radio frequency, microwaves, and so on, to the gas, and plasma is often called gas discharges because passing an electrical discharge through the gas is a most common way to produce it.

Plasma that is not in any local thermodynamic equilibrium is called cold plasma. In this plasma, thermodynamic equilibrium is not reached between electrons and heavy particles even at a local scale in low-pressure discharges. The temperature of the electrons is much higher than that of the heavy particles and the electrons can reach temperatures of 10^4-10^5 K, while the temperature of the gas can be as low as room temperature. Because ions, atoms and molecules cannot interchange heat with electrons and electrons travel much faster than them, these spices are kept almost at room temperature. As a consequence this plasma might present temperatures similar to room temperature.

There are many internal parameters and external parameters to define plasma characteristics for any kind of cold plasma systems when treating powders. The internal parameters of the plasma system are determined by the external parameters shown in Table 2-1, and external parameters are what applied to the plasma reactor operation conditions.

13.56 MHz radiofrequency is mostly used as the source to generate electrical field in the plasma system, and electrodes can be either placed inside or outside part of the plasma reactor. Inner electrodes are for the case of metallic reactor and outer electrodes are for the Pyrex and quartz reactors. The electrodeless (outer electrodes) is proffered when treating powder materials to avoid the direct contact of powders with electrodes, such as a copper coil inductively coupled or outer electrodes capacitively couples to the generator. A matching box is needed in all of cases in order to effectively generate plasma and minimize the reflected power.

Worth to note that any surface inside the plasma is covered by an electron sheet to develop a negative bias, and the plasma bulk will definitely has a higher potential than the surface. Therefore the positive energetic ions will accelerated to the surface to produce etching or surface ablation effect, which seems good for powders' surface cleaning.

Table 2-1 Internal and External Parameters in a Plasma System [12]

Internal Parameters	External Parameters
• Fragmentation degree of the gas • Density of neutrals • Density of electrons and electron Energy Ionization degree • Residence time of the species • Process homogeneity • Positive ion bombardment, sputtering • Deposition, etching, treatment rate • Contaminations	• Pressure • Feed composition, flow rate, leaks • Field frequency • Power density • Reactor configuration, materials, electrode geometry • Substrate position • Duty cycle %, time on, time off in pulsed plasmas • Substrate temperature • Substrate bias potential

Position of sample is also important factor to be taken into consideration. Samples can be either placed in the plasma bulk zone, where the plasma generated, in which plasma shows a strong ion bombardment effect, or placed remote to the plasma generation region, in which bombardment effect reduced a lot and less severe treatment.

There are two forms of oleic acid (surfactant) on the synthesized nanoparticles: Free oleic acid and oleic acid bonded on the surface to form carboxylate. For example, during the surfactant-assisted milling of the RE–Co powders, the OA molecule is attached to the particle in carboxylate form, Figure 2-3. [8] Oleic acid attached on nanoparticles in the carboxylate form could not be washed away in solvents by ultrasonic and centrifugal machine, while free oleic acid can be easily washed away. [10] Chemical solvent or annealing method works for removing oleic acid but magnetic nanoparticles would be damaged. The RF cold plasma has advantages over above methods as the plasma temperature is less than 373K so decomposition of surfactant can be avoided, and the energetic Argon ions could strike away organic molecules on the surface of metal while magnetic nanoparticles could not chemically react with argon ions. The work in this thesis tried to find out if cold plasma works for nanoparticles surface cleaning. [10, 24-28]

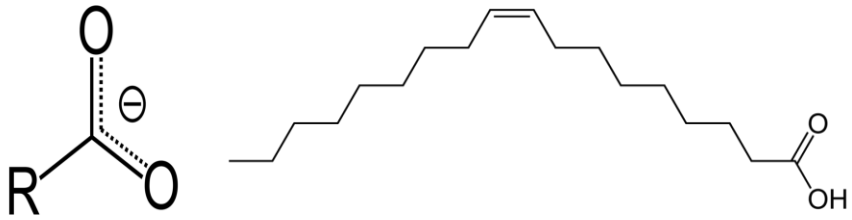

Figure 2-3 Diagram of a carboxylate ion (Left), R is an organic group, and a free oleic acid molecule (Right) [32-33]

2.2.2 Principles of Argon Cold Plasma Cleaning

$SmCo_5$ nanoflakes are easy to get oxidized, so argon plasma is used for cleaning their surfaces because it removes almost all kinds of contamination through ion bombardment (etching effect) without causing a chemical reaction or oxidation on the surface of the substrate. Because any surface in the plasma is covered by an electron sheet developing a negative bias, plasma bulk has a higher potential than the surface of

samples in the reactor. Activated ions, which is positive, and combine with the fact that due to long mean free path at very low pressure in plasma, they will gain sufficient energy behaving like a molecular sandblast to break down organic bonds. These contaminants are again vaporized and evacuated from the chamber during processing, because of the pumping system connected to reactor. The working pressure should be around several hundred mTorr or even less, and the base pressure is about 5 mTorr through hours of pumping. The reasons why low pressure is needed are as follows: at lower pressure the coefficient of heat transfer is decreased, the ion energy sufficiently increases due to long mean free path so ions become more effective in breaking organic chemical bonds. Besides, because of long mean free path, there will be fewer collisions among particles in the plasma, and this is good to maintain the plasma state. [12, 24-28]

2.2.3 Experimental Set-up for Cold Plasma Treatment [30-31, 34]

The plasma reactor chamber was a cylindrical-like reactor with 5 cm inner diameter, 46 cm length two stopcocks at both ends and a clamp. The reactor was made of borosilicate glass (Pyrex). The inlet and outlet were connected to hollow shaft cartridge mount Ferrofluidic feedthroughs (Ferrotec, Model-HS5 00SLXC), which enabled the plasma reactor to rotate freely and continuously under vacuum. A live electrode was located outside and underneath along the length of the reactor, while the ground electrode was placed on top of the reactor. (Figure 2-5)

The RF system consisted of a 300 W RF amplifier (ENI, Model-A300), a pulse generator (Tetronix, Model-2101), a function generator (Wavetek, Model-166), a frequency counter (Hewlett Packard, Model-5315A) and an in-house made capacitance/inductance matching network. Plasma treatments were conducted at the RF frequency of 13.56 MHz. An exhaust valve controller (MKS, Model 252E-1-VPO) monitored the pressure inside the reactor and controlled a butterfly valve (MKS Model

253B-1-40-1) positioned downstream, which was employed to adjust the pressure inside the reactor. The system was evacuated by a mechanical rotary vacuum pump (Leybold, Model D16B). Typically, background pressure was pumped down to 5 mTorr before the argon gas (ultra high purity) was introduced into the plasma reactor to avoid contamination from other molecules. A liquid nitrogen cold trap was placed after plasma reactor and before the vacuum pump products that escaped from plasma reactor thus preventing these molecules from flowing into the vacuum pump. A schematic diagram of the plasma reactor is provided in Figure 2-4.

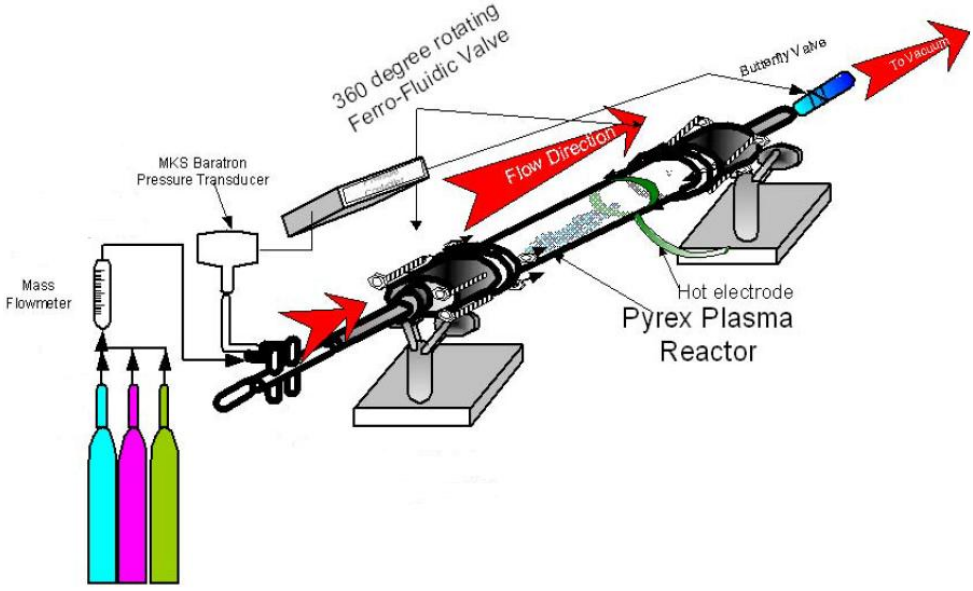

Figure 2-4 Schematic diagram of the rotary plasma reactor system employed for the nanoparticles surface cleaning [34]

Because $CoFe_2O_4$ nanoparticles are not very easy to get oxidized in the air, ordinary glass reactor was used. Grooves on the inner side of glass reactor would help stir particles when the glass reactor rotates. Glass beads were mixed with nanoparticles to help stir the nanoparticles. By stirring the nanoparticles they were more likely to get

homogeneous plasma treatment. There is no need to keep the glass reactor to be airtight after plasma treatment when dealing with $CoFe_2O_4$ nanoparticles.

When treating $SmCo_5$, a new glass reactor (Figure 2-6) was specially designed and this is because $SmCo_5$ powders are easy to get oxidized when exposed in the air. Therefore, after the plasma treatment the glass reactor should be airtight before it is taken off from the plasma system and transferred into glove box. Two stopcocks are part of this reactor which will make the glass reactor airtight after plasma treatment. The flanges are applied so the samples can be loaded inside the glass reactor.

Figure 2-5 Picture of the rotary plasma reactor with electrodes outside of the glass reactor

After the plasma treatment, two stopcocks would be closed so the glass reactor became airtight. Powders can be loaded into or be taken out from the reactor by opening the clamps part. The grooves on the glass reactor and glass beads inside the glass reactor were used to help stir the powders to obtain homogenous treatment in the plasma process (Figure 2-7).

Figure 2-6 the newly designed glass reactor for plasma treatment of SmCo powders

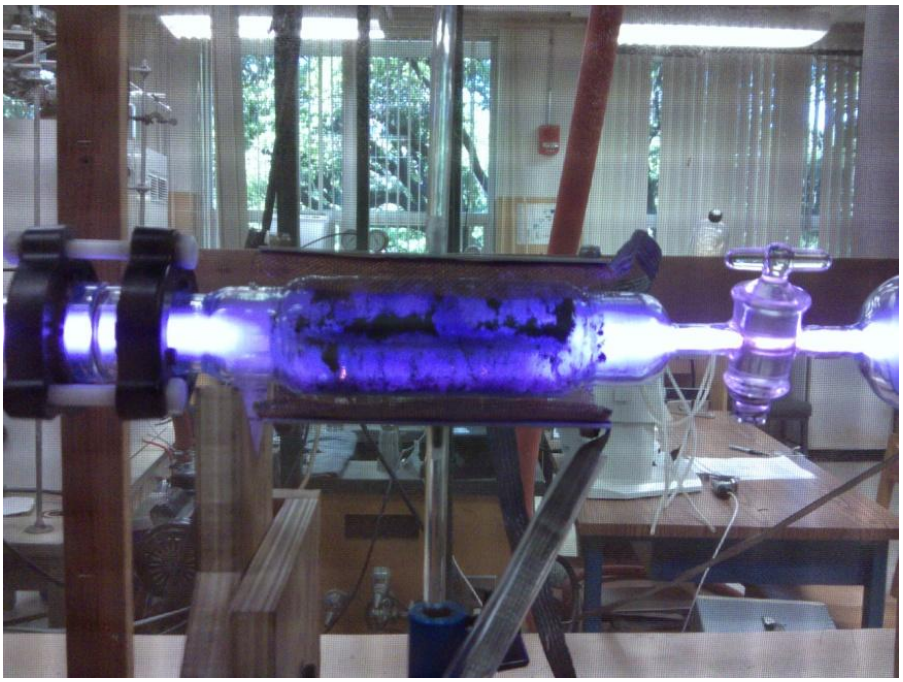

Figure 2-7 The picture of the glass reactor under plasma treatment

2.2.4 Experimental Details for Cold Plasma Cleaning

2.2.4.1 $CoFe_2O_4$ nanoparticles

3 g chemical synthesized $CoFe_2O_4$ nanoparticles washed in ultrasonic bath (repeated for 8 times) by organic solvents was plasma treated for 120 min. The pressure was kept at 120 mTorr and the power was 250 W. The oleic acid bonded on the surface was characterized by FTIR and XPS.

2.2.4.2 $SmCo_5$ nanoflakes

In this work, firstly, 6 g ball-milled $SmCo_5$ washed by organic solvents had been plasma treated for 30 minutes, under the pressure of 150 m Torr and with a power of 150 W. After comparison of the XPS and XRD results between the untreated and 30 minutes treated samples, the 30 minutes treated samples were then further treated with the same parameters and the total plasma treatment time was up to 180 minutes. Then the 180 minutes treated sample was characterized to see the carbon content change on the surface and phase change. The above experiments was tried to verify whether cold plasma method works for cleaning.

The following steps of this work is tried to find the best parameters for cold plasma cleaning. The first batch of samples was treated under different pressure and the parameters are shown below in the tables 2-2.

Table 2-2 The Parameters for Plasma Treatment of the Samples under Different Pressure

Sample number	Pressure(mTorr)	Power(W)	Treating time(min)
1(untreated)	N/A	N/A	N/A
2	150	150	60
3	250	150	60
4	350	150	60
5	450	150	60

The second batch of samples was treated under different time and other parameters were kept the same, Table 2-3.

Table 2-3 The Parameters for Plasma Treatment of the Samples under Different Treating Time

Sample number	Pressure(mTorr)	Power(W)	Treating time(min)
6(untreated)	N/A	N/A	N/A
7	250	150	10
8	250	150	30
9	250	150	60
10	250	150	120
11	250	150	180

2.3 Characterization of Plasma Treated Magnetic Nanoparticles

2.3.1 XPS and FTIR [30]

The nanoparticle surface compositions were quantitively characterized mainly by using X-ray photoelectron spectroscopy (XPS). The XPS spectra were obtained on a Perkin-Elmer PHI 5000 series spectrometer equipped with an X-ray source monochromator. The X-ray source employed is an Al Kα at 1486.6 eV. A pass energy of 17.90 eV, giving a resolution of 0.6 eV with Ag ($3d_{5/2}$), was used. Spectra were usually obtained at a pass energy of 8.95 eV using a 45º take-off angle. An electron flood gun (neutralizer) was employed to neutralize charge build-up on the insulator type films produced in the plasma deposition. The electron gun was operated under conditions to provide optimum resolution of the C (1s) peaks. Typical operating conditions for the neutralizer were 22.0 mA emission current and 1.8 eV electron energy. The XPS spectra of the plasma polymer films were standardized by centering the lowest binding energy peak in the C (1s) multiplets to 284.6 eV, which represents the binding energy of C atoms bonded exclusively to other C or H atoms.

Quantitative analysis of elemental compositions of organic coatings was achieved by XPS analysis in a low-resolution survey scans. The atomic concentrations of surface elements were obtained by measuring the peak areas of the inner-level electrons, coupled with known instrument sensitivity factors for each element.

A Bruker Vector 22 FT-IR spectrophotometer was employed (ATR mode) for infrared analysis. FT-IR spectra were recorded at $8cm^{-1}$ resolution and 64 scans of $SmCo_5$.

2.3.2 X-ray Diffraction (XRD)

Philips PW 1710 Diffractometer with Cu-Kα radiation (wavelength λ=1.54056 A^o) was used for studying the crystallinity of the samples. The samples were prepared by depositing them on glass substrate.

Chapter 3

Results and Discussion

3.1 Experiments to Cleaning Surfactant on $CoFe_2O_4$ Nanoparticles

$CoFe_2O_4$ nanoparticles with surfactant(OA) have been treated via cold plasma under different conditions. The FTIR and XPS measurements indicate that the OA surfactant can be partly removed from the particle surface.

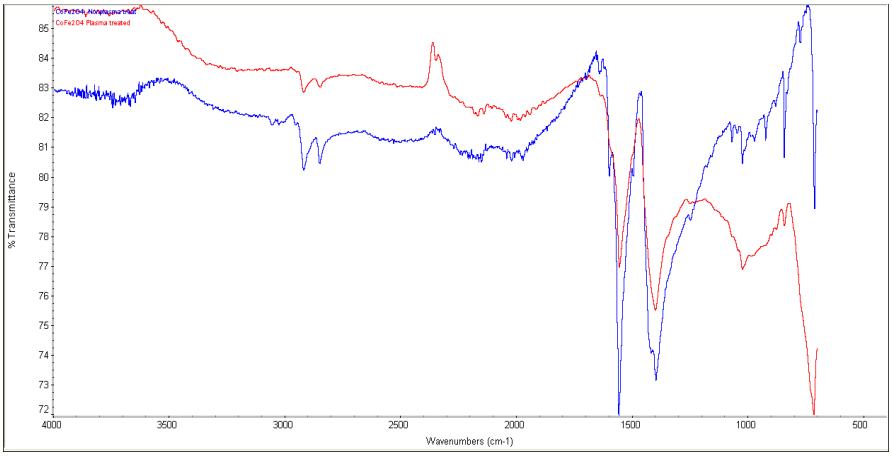

Figure 3-1 FTIR (ATR) result of oleic acid on cobalt ferrite nanoparticles before (Blue) and after (Red) plasma treatment

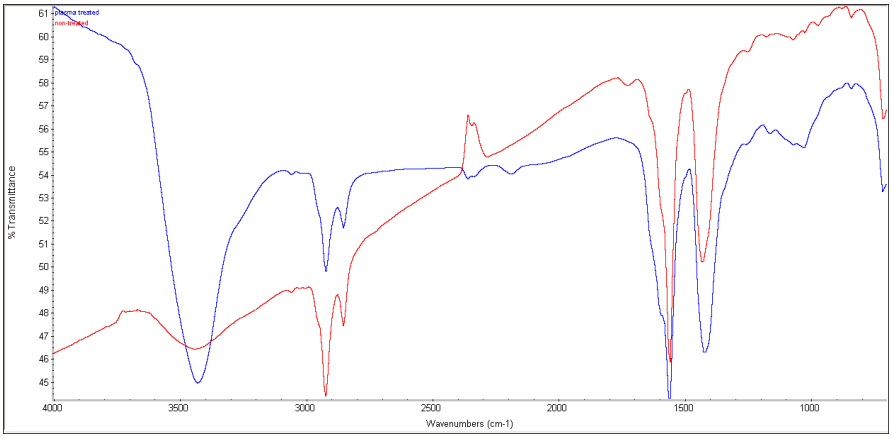

Figure 3-2 FTIR (Transmission) result of oleic acid on cobalt ferrite nanoparticles before (Red) and after (Blue) plasma treatment

FTIR result shows there is still some oleic acid left on the surface of the nanoparticles even after a plasma treatment for 120 minutes. Both Attenuated Total reflectance (ATR) (Figure 3-1) and transmission mode (Figure 3-2) of FTIR technique were used to detect the organic surfactants on nanoparticles. The two peaks in the region of wavelength between 2800 and 3000 cm^{-1} correspond to C-H bond, while the two strong peaks close to 1500cm^{-1} are the finger print of Carboxylate bond.

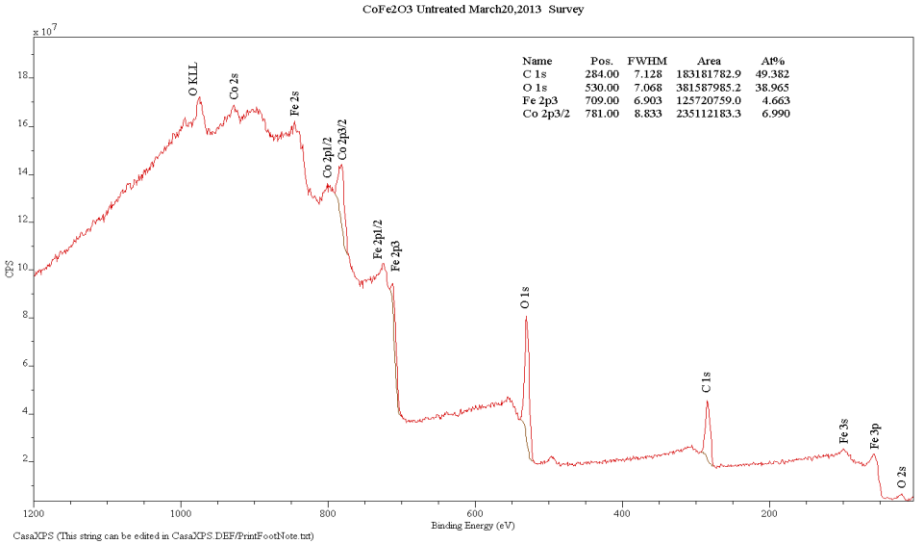

Figure 3-3 XPS result of surface composition on cobalt ferrite nanoparticles before plasma treatment

The fact that oleic acid was left on the surface of plasma treated nanoparticles can be further confirmed by XPS result. By comparing the XPS results of nanoparticles before (Figure 3-3) and after plasma (Figure 3-4) treatment, atomic percentage (At %) of Carbon decreased from 49.3 to 32.2, Oxygen decreased from 38.9 to 26.5. This results shows that cold plasma can partly remove surfactant on cobalt ferrite nanoparticles. However, other elements such as Si and F were introduced on the surface of nanoparticles. It is probable that the powerful ion bombardment could even break the

surface of the glass reactor, and the atoms that were stroke away from the surface of glass reactor moved to the nanoparticle surface.

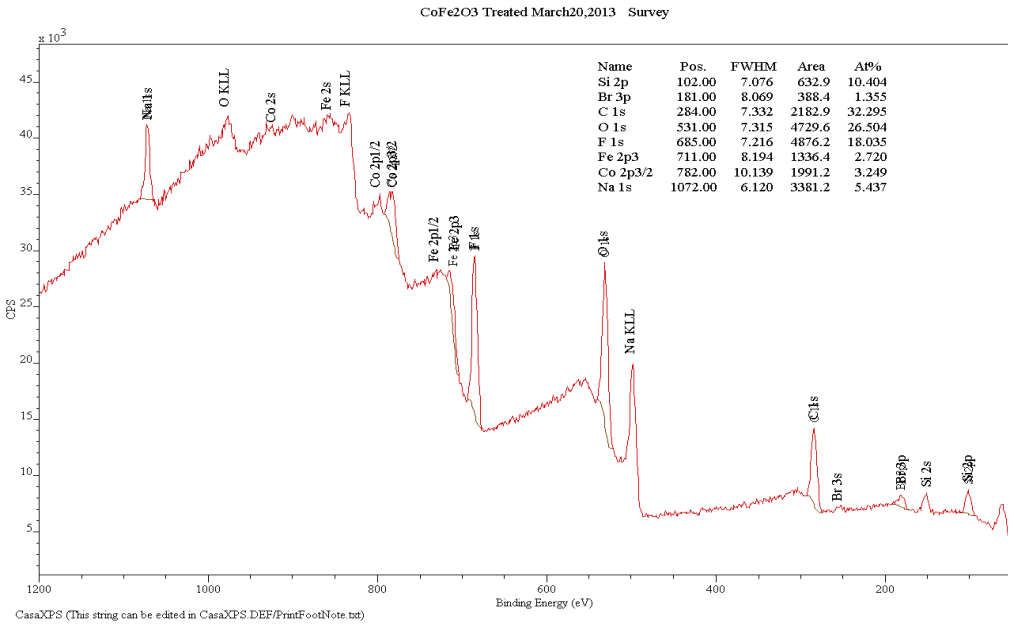

Figure 3-4 XPS result of surface composition on cobalt ferrite nanoparticles after plasma treatment

3.2 Experiments to Plasma Cleaning Surfactants on $SmCo_5$ Nanoflakes

3.2.1 Experiments to Confirm the Effect of Plasma Cleaning

For the first batch of samples, experiments were designed to check the effect of cleaning in plasma treatment. Ball-milled $SmCo_5$ nanoflakes were washed for eight times in order to remove the free oleic acid left on their surface. The experimental results indicated that the cold-plasma can at least partly remove OA surfactants on $SmCo_5$ nanoflakes.

Table 3-1 displays the XPS results for the cold plasma treated- and untreated-$SmCo_5$ nanofalkes. The results (Figure 3-5) indicated that the content for C 1s is 67.0%at, and these for the Sm $3d_{5/2}$ and Co $2p_{3/2}$ are1.0%at, and 5.1%at, respectively. After 30

minutes of argon plasma treatment, according to XPS result (Table 3-1), the content for C 1s decreased to 57.7%at, while the content for both Sm $3d_{5/2}$ and Co $2p_{3/2}$ increased by a little amount. The content of Sm $3d_{5/2}$ was increased to 5.2%at and that of Co 2p3/2 was increased to 7.2%at. In Table 3-1, the intensity for C 1s decreased while these for both Sm $3d_{5/2}$ and Co $2p_{3/2}$ were increased a little. This can be explained as with plasma treatment, some carbon atoms were removed from the surface and in the mean time more Sm and Co atoms were exposed on the surface with the number decreasing of carbon atoms.

Table 3-1 Atomic Percentage (At %) Change with Different Treating Time on $SmCo_5$ Nanoflakes from XPS Results

Treating Time / Element name	Untreated	30min	180min
C 1s	67.0	57.7	30.6
Sm $3d_{5/2}$	1.0	5.2	17.2
Co $2p_{3/2}$	5.1	7.2	6.8
Sm $3d_{5/2}$+ Co $2p_{3/2}$	6.2	12.6	24.0

Table 3-2 The Content Ratio Change of C1s/Sm $3d_{5/2}$, and C1s/(Sm $3d_{5/2}$ + Co $2p_{3/2}$) with Treating Time on $SmCo_5$ Nanoflakes from XPS Results

Treating time / At% Ratio	untreated	30min	180min
C 1s/ Sm $3d_{5/2}$	62.2	10.7	1.7
C 1s/ (Sm $3d_{5/2}$+ Co $2p_{3/2}$)	10.8	4.5	1.2

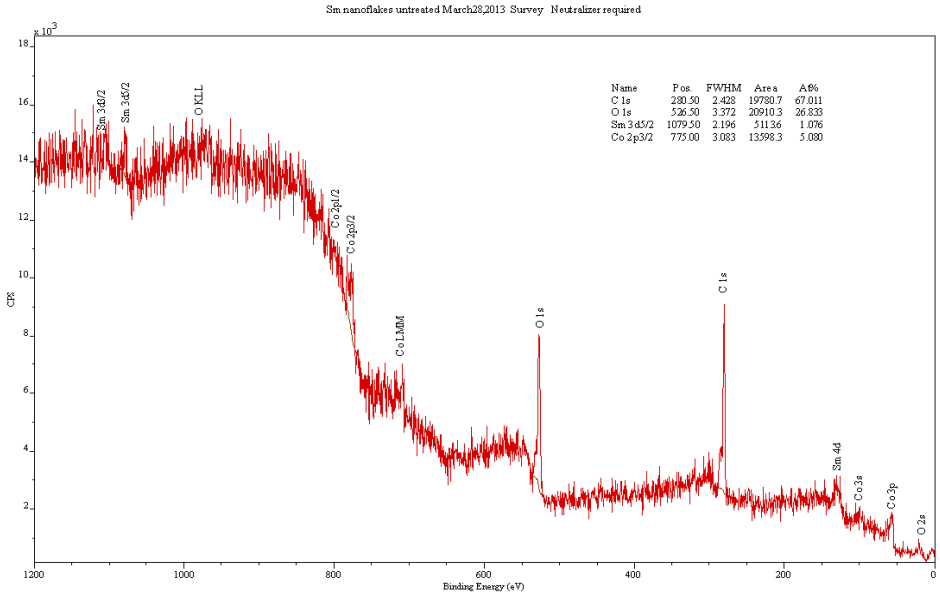

Figure 3-5 XPS result of surface composition on $SmCo_5$ nanoflakes before plasma treatment

By further plasma treating the same sample, with a total treating time of 180 minutes, the carbon content was tremendously reduced according to the XPS result. In Table 3-1, the At% of C1s was cut in half and the Sm $3d_{5/2}$ was tripled when compared with the result of 30 minutes treatment. The intensity of Sm $3d_{5/2}$ peaks increased and for C 1s it decreased tremendously. The XPS results showed that with a treatment of 180 minutes (Figure 3-6), when compared with those untreated (Figure 3-5), the cleaning is effective because carbon content decreased a lot and meanwhile much more Sm atoms were exposed to the environment. The content Ratio of C1s/Sm $3d_{5/2}$, and C1s/(Sm $3d_{5/2}$ + Co $2p_{3/2}$), compared with the untreated, also decreased a lot for the sample with treatment time of 180 minutes (Table 3-2). The results indicate that after plasma treatment the relative number of Carbon atoms decreased while the relative number of Samarium atoms increased. In fact, the surface of the nanoflake would inevitably absorb CO_2 in the air before the XPS characterization, especially for the samples after plasma

treatment (due to the formation of clean and active surface). Because XPS is a very sensitive surface characterization technique, the carbon content from the XPS results must be higher than the ones without being exposed to the air. Therefore, the real effect should be better than what the XPS results displayed here.

TGA result (Figure 3-7) showed that for plasma-treated samples, they gain weight more quickly than those samples without plasma treatment. The reason is that the cleaned surface of the plasma treated samples is more easily to get oxidized to gain weight during TGA measurement. Untreated samples did not gain weight quickly because the surfactant on the surface prevented the oxygen atoms to react with metal surface. There was a slow drop stating around 60 degree for untreated samples, this is because some ethanol haptane evaporated at higher temperature. The TGA results also showed that plasma works for surface cleaning.

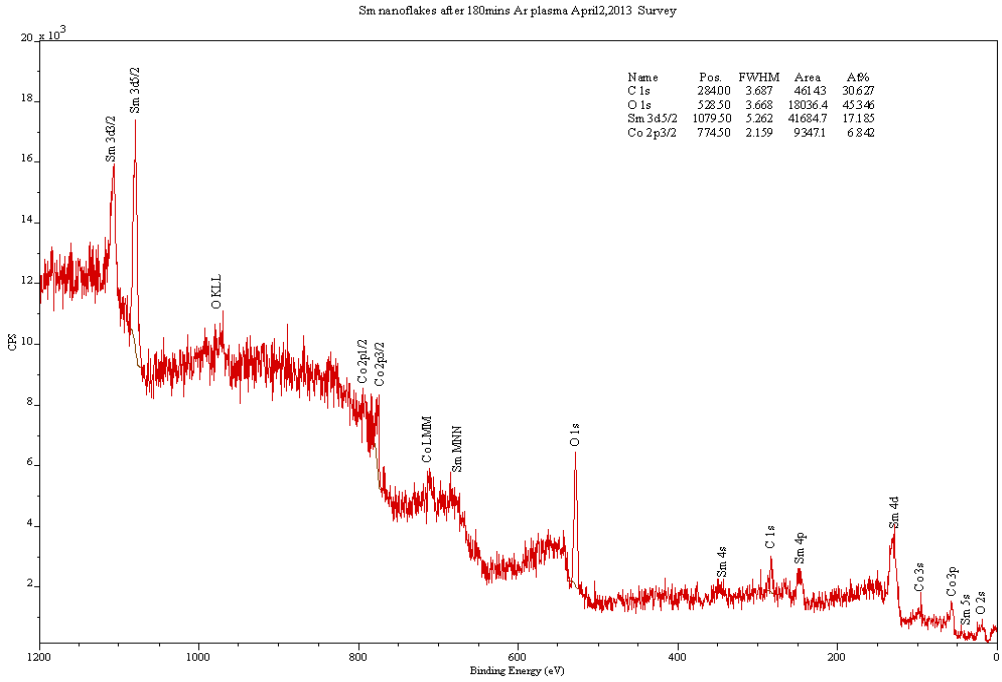

Figure 3-6 XPS result of surface compositon on $SmCo_5$ nanoflakes after plasma treatment for 180 minutes

One thing has to be noted is the decomposition happened after long treatment time. XRD result showed that with a treatment of 180 minutes, part of $SmCo_5$ nanoparticles was decomposed, as can be seen from cobalt peak appearing in Figure 3-8. When treating Fe and $SmCo_5$ nanoparticles, after a continuous treatment of around 10 minutes, some spots in the sample became very bright (see Figure 2-7). The 'spark' did not happen when treating cobalt ferrite nanoparticles. The occurrence of sparks is probably related with the low electrical resistivity of these nanoparticles. For Fe and $SmCo_5$, their electrical resistivity are around 1.0×10^{-9} Ω·cm and $5\sim6\times10^{-5}$ Ω·cm, respectively. The low electrical resistivity is responsible for the occurrence of sparks in these samples. On the other hand, the electrical resistivity of $CoFe_2O_4$ is up to 108 Ω·cm, which showed no sparks during plasma-treatments.

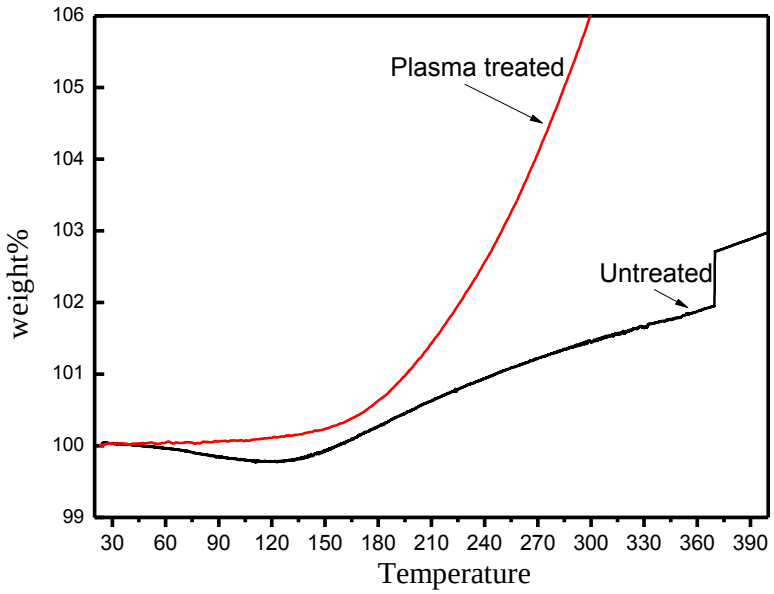

Figure 3-7 TGA results of ball-milled $SmCo_5$ nanoparticles before and after plasma treatment (30min)

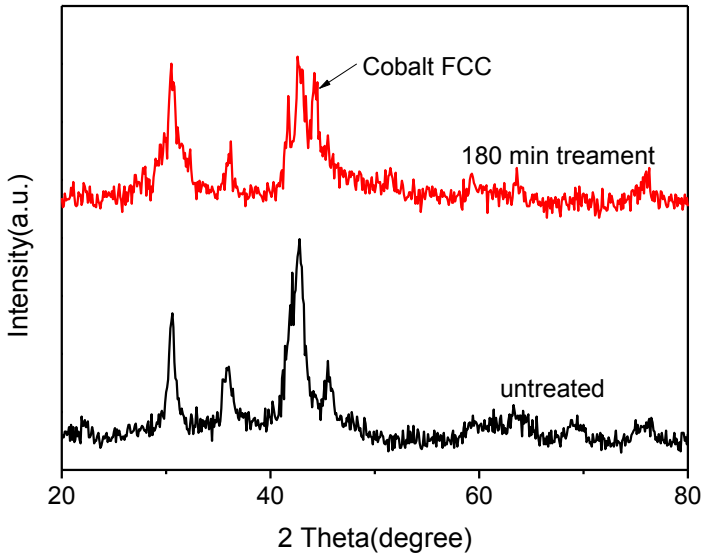

Figure 3-8 X-ray diffraction patterns of untreated and plasma-treated (180 min) ball-milled $SmCo_5$ nanoflakes

In details, the phenomena of sparks can be explained as following: the organic coating was almost completely removed from the nanoparticle surface by plasma and thus the metal surface was exposed to plasma. For metal nanopaticles with a very low electrical resistivity, heat from electrons, typically with very high temperature and energy from ions bombardment can be conducted easily on those spots, which will bring a local high temperature to make sparks happen. Because of high local temperature those spot or particles appeared like “spark” with bright color. The sparks did not happen when treating cobalt ferrite nanoparticles and this is probably because cobalt ferrite has a very high electrical resistivity.

There are some ways to reduce sparks such as cooling down the glass reactor for 30 minutes after running plasma for 5 minutes. Powerful fans were used in the whole process to bring outside cooling of glass reactor to reduce the temperature in the

powders. Pulsed plasma, instead of continuous plasma was used to reduce the temperature in the glass reactor and thus reduce sparks. By applying above methods, when treating $SmCo_5$ nanoparticles, the time span before sparks happening can be extended: typically after a treatment time of around 60minutes. While for the continuous plasma treatment, sparks began to appear in less than 10 minutes. However, even above tricks were applied, when plasma treating time is long enough, typical 100 minutes or more for treating $SmCo_5$ nanoparticles, sparks appeared shortly after the powder is turned on, even if with an enough time of cooling was applied to nanoparticles inside glass reactor.

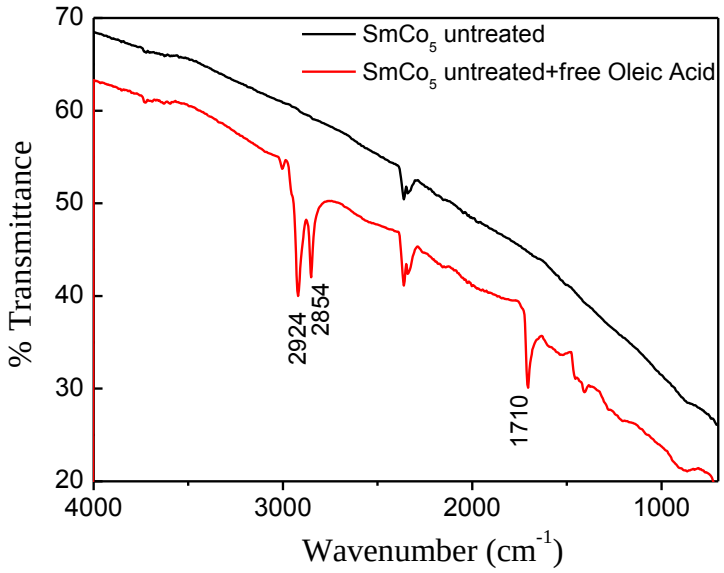

Figure 3-9 FTIR (ATR mode) result of OA on untreated ball-milled $SmCo_5$ nanoflakes and untreated $SmCo_5$ nanoflakes with free oleic acid

Fourier Transform Infrared Spectroscopy (FTIR) was utilized to characterize the oleic acid on the surface of ball-milled $SmCo_5$ nanoflakes. First the Attenuated Total Reflectance (ATR) mode of FTIR was used. From the results of untreated $SmCo_5$

nanoparticles (Figure 3-9) no peaks could be found in the region between 2500 and 3000 (cm^{-1}), or any peaks around 1500(cm^{-1}), which corresponds to C-H, and C=O bond, respectively.

For the same sample, two drop of free oleic acid was added and was mixed with the ball-milled $SmCo_5$ nanoflakes, however, the results obtained by FTIR-ATR is very different. Two sharp bands at 2924 and 2854 cm^{-1} were attributed to the asymmetric CH_2 stretch and the symmetric CH_2 stretch, respectively. The intense peak at 1710 cm^{-1} was derived from the existence of the C=O stretch. By comparing with the standard FTIR pattern of free oleic acid, this result is exactly match with the standard results, and the peak intensity is good.

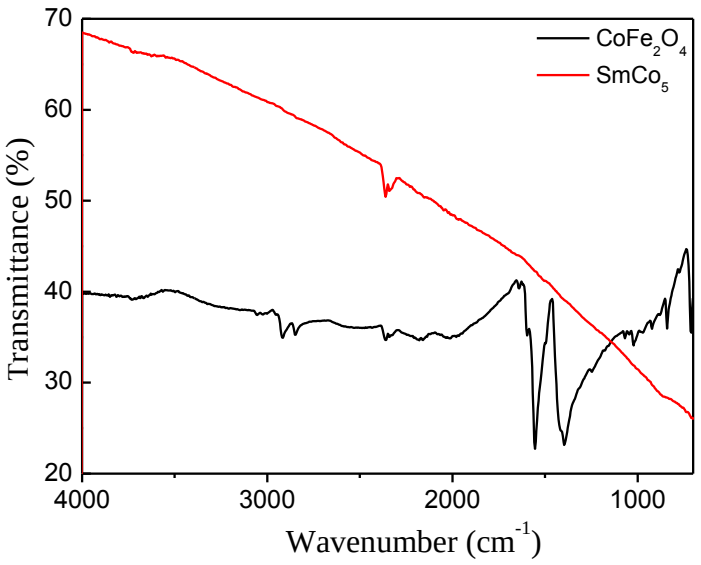

Figure 3-10 FTIR (ATR mode) result of OA on untreated ball-milled $SmCo_5$ nanoflakes and cobalt ferrite nanoparticles

Ball-milled $SmCo_5$ nanoflakes have length of about 200 micron meters and thickness of 10 nanometers. As for $CoFe_2O_4$ nanoparticles, they are particles with a

diameter of 10-20 nanometers. Thus $SmCo_5$ nanopartiles are thousands time larger than $CoFe_2O_4$ nanoparticles, which means high ratio of surface area for these particles and more oleic acid on cobalt ferrite nanoparticle surface. The amount of oleic acid on $SmCo_5$ nanoparticles is too scarce to be detected by FTIR. For chemical synthesized cobalt ferrite nanoparticles, oleic acid is also bonded on the surface and could not be washed away by ethanol and heptanes. Same technique to characterize the oleic acid on their surface was used, FTIR-ATR technique. From the result (Figure 3-10) we could see the peaks in the region of 2800-3000 cm^{-1}, which is C-H bond, and intense peaks at around 1500 cm^{-1}, which is different than the C=O bond peak in Figure 3-9, as these two peaks corresponds to carboxylate bond.

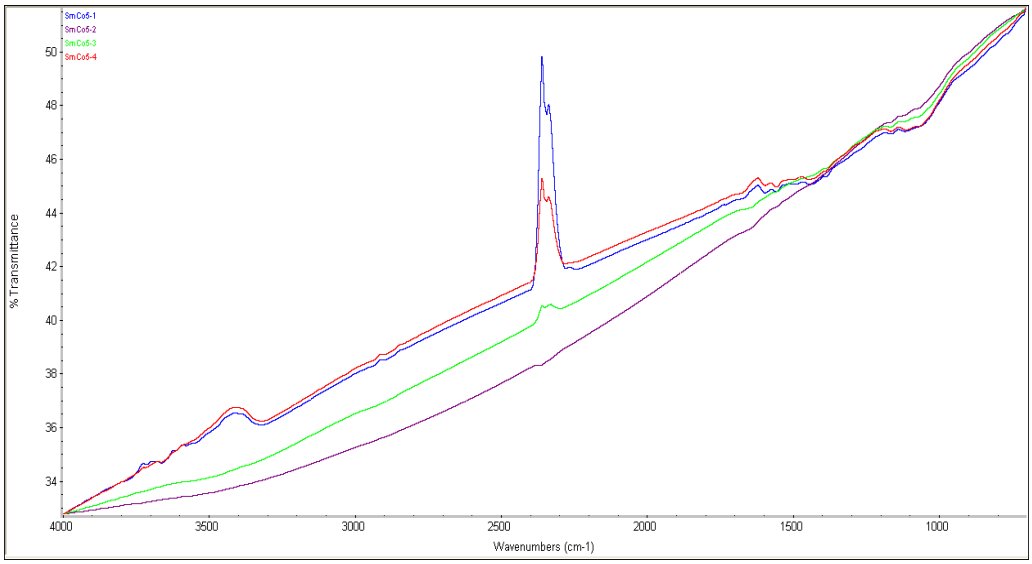

Figure 3-11 FTIR (Transmission mode) result of untreated ball-milled $SmCo_5$ nanoflakes (Four times of measurement for the same sample)

FTIR transmission mode was also tried. Samples were mixed with KBr and compressed into a pellet. Ball-milled $SmCo_5$ nanoflakes were characterized for four times

but still no characteristic peaks belong to oleic acid could be found on the curves (Figure 3-11). However, this technique also works on cobalt ferrite. This agrees with the discussion above that such trace amount of organic materials on $SmCo_5$ nanoparticles could not be detected by FTIR.

4.2.2 Effect of Pressure on Plasma Cleaning

To understand the effect of the plasma treatment Ar pressure on cleaning, the second batch of samples was treated under different pressure. XRD results (Figure 3-12) of the untreated $SmCo_5$ and plasma-treated $SmCo_5$ nanoflakes under different pressure showed that there was no phase change after plasma treatment, all the x-rays patterns agrees with the $SmCo_5$ peaks from PDF database. It also means with a treatment of 60 min, even under different pressure, the $SmCo_5$ did not experience any decomposition as the temperature during plasma treatment is not high.

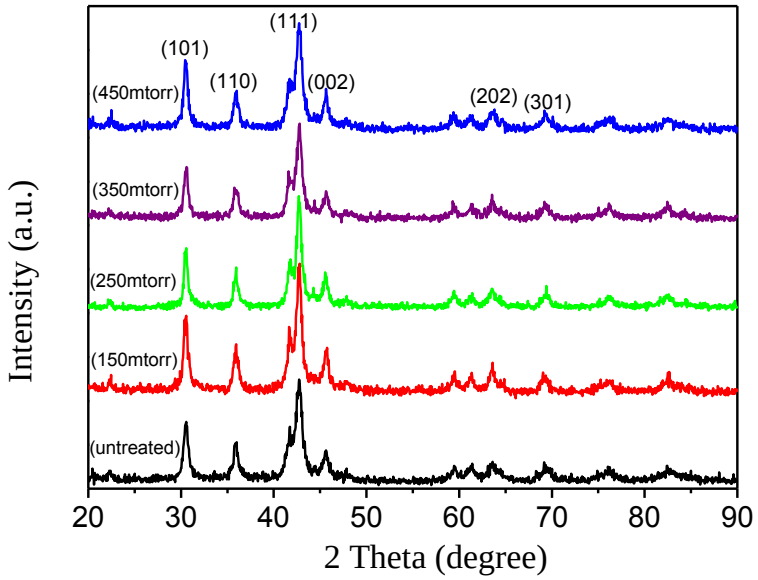

Figure 3-12 X-ray diffraction patterns of untreated and plasma-treated (under different pressure) $SmCo_5$ nanoflakes

Figure 3-13 shows the percentage of atomic number change for C 1s, Sm $3d_{5/2}$, Co $2p_{3/2}$ and Sm $3d_{5/2}$+Co $2p_{3/2}$ and the data was from the XPS results. This gives 250 mTorr as the most effective pressure in plasma cleaning. This is because under the pressure 250 mTorr on the surface of the nanoflakes there were relatively less percentage of Carbon atoms but more metal atoms such as Sm and Co. The reason why Oxygen content did not decrease, from XPS results, can be explained as that $SmCo_5$ nanoflakes is very easy to be oxidized in the air, and this is the reason why more oxygen atoms was introduced(before XPS characterization).

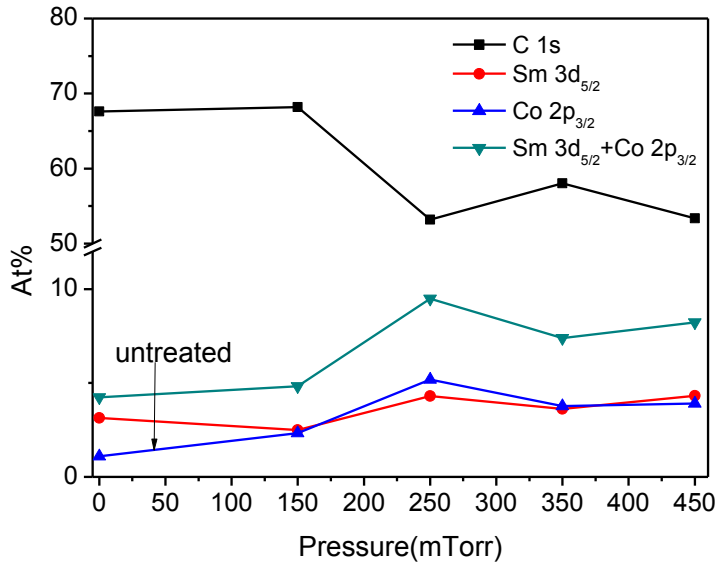

Figure 3-13 At % change of C 1s, Sm $3d_{5/2}$, Co $2p_{3/2}$ and Sm $3d_{5/2}$+Co $2p_{3/2}$ with different treating pressure

3.2.3 Effect of Treating Time on Plasma Cleaning

As shown in Fig 3-12, there was no phase change when nanoparticles were treated for 60 minutes, even under different pressure. However, from the XRD results of $SmCo_5$ that was treated under different treating time (Figure 3-14), Cobalt (FCC) peak

started to appear in the x-ray patterns that corresponds to the treating time of 120 min and in 180 min the peak intensity increased. This is probably due to the sparks occurrence when the treating time is long enough, typically over 60 minutes, which the local temperature of the sparks was very high so that $SmCo_5$ nanoflakes were partly decomposed.

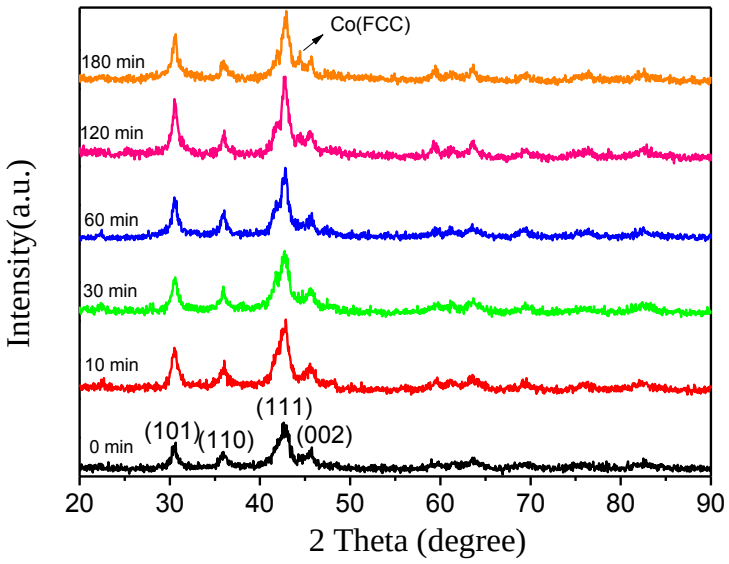

Figure 3-14 X-ray diffraction patterns of untreated and plasma-treated (under different treating time) $SmCo_5$ nanoflakes

Figure 3-15 shows the content change for C 1s, Sm $3d_{5/2}$, and Co $2p_{3/2}$ with different treating time derived from the XPS results. Those results were strange as with longer treating time the Carbon content even increased. Those results did not agree with what is expected to happen: Carbon content decreased with increasing treating time. For the previous treatment with a treating time of 180 minutes the carbon atomic percentage decreased from 67.0 to 30.6, and increased from 1.0 to 17.2 for Sm $3d_{5/2}$. While from the

results in Figure 3-15, C 1s decreased less than 10 percent and for Sm $3d_{5/2}$ it only increased a little, around 5 percent.

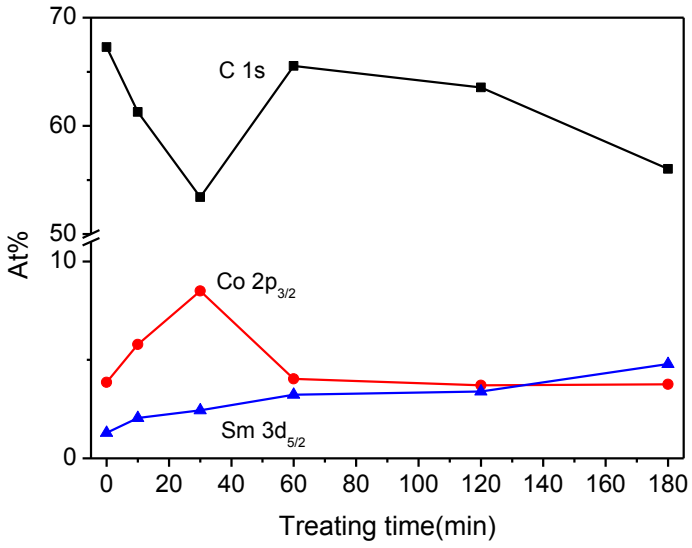

Figure 3-15 At % change of C 1s, Sm $3d_{5/2}$, and Co $2p_{3/2}$ with different treating time

The possible explanation is that the agglomeration happened in the nanoparticles during the plasma treatment, which yielded an inhomogeneous plasma treatment and big difference between different XPS results. Further work is highly needed to clarify these behaviors.

Chapter 4

Summary

Plasma cleaning of nanoparticle surface has been performed successfully. Sparks can be reduced by controlling the powders temperature from (cooling down after 5 min treatment, outside cooling, pulsed plasma).Further works needed to find out more effective conditions for the treatment and characterization.

FTIR and XPS results indicate that the OA surfactant can be partly removed from the $CoFe_2O_4$ particle surface via Argon cold plasma treatment. FTIR results, from both Attenuated Total reflectance (ATR) and transmission modes, showed there is still some oleic acid left on the surface of the $CoFe_2O_4$ nanoparticles even after a plasma treatment for 120 minutes. XPS results showed atomic percentage (At %) of Carbon decreased from 49.3 to 32.2 with a treatment of 120 minutes. However, other elements such as Si and F were introduced on the surface of $CoFe_2O_4$ nanoparticles. It is probable that the powerful ion bombardment could even break the surface of the glass reactor, and the atoms that were stroke away from the surface of glass reactor moved to the nanoparticle surface.

As with the Argon cold plasma treatment of $SmCo_5$ nanoparticles, XPS results showed with a total treating time of 180 minutes the cleaning is effective because carbon content decreased a lot and meanwhile much more Sm atoms were exposed to the environment. Due to the fact that the surface of the $SmCo_5$ nanoflakes would inevitably absorb CO_2 in the air before the XPS characterization, especially for the samples after plasma treatment (lead to the formation of clean and active surface), and XPS is a very sensitive surface characterization technique, the carbon content shown on the XPS results must be higher than the what the real effect reflected. TGA results agreed with the cleaning effect that for plasma-treated samples, they gain weight more quickly than those

samples without plasma treatment. The reason is that the cleaned surface of the plasma treated samples is more easily to get oxidized to gain weight during TGA measurement.

Decomposition of nanoparticles happened when treating Fe and $SmCo_5$ nanoparticles. Some spots in the samples became very bright during the plasma treatment. The ‘spark’ did not happen when treating cobalt ferrite nanoparticles. The occurrence of sparks is probably related with the electrical resistivity of these nanoparticles. The electrical resistivity for Fe and $SmCo_5$ is much less than that of $CoFe_2O_4$ nanoparticles. The phenomena of sparks can be explained as following: the organic coating was almost completely removed from the nanoparticle surface by plasma and thus the metal surface was exposed to plasma. For metal nanopaticles with a very low electrical resistivity, heat from electrons, typically with very high temperature and energy from ions bombardment can be conducted easily on those spots, which will bring a local high temperature to make sparks happen. Because of high local temperature those spot or particles appeared like “spark” with bright color. The sparks did not happen when treating cobalt ferrite nanoparticles and this is probably because cobalt ferrite has a very high electrical resistivity. There are some ways to reduce sparks such as cooling down the glass reactor for 30 minutes after running plasma for 5 minutes. Powerful fans were used in the whole process to bring outside cooling of glass reactor to reduce the temperature in the powders. Pulsed plasma, instead of continuous plasma was used to reduce the temperature in the glass reactor and thus reduce sparks. By applying above methods, when treating $SmCo_5$ nanoparticles, the time span before sparks happening can be extended: typically after a treatment time of around 60minutes. While for the continuous plasma treatment, sparks began to appear in less than 10 minutes. However, even above tricks were applied, when plasma treating time is long enough, typical 100 minutes or more for treating $SmCo_5$ nanoparticles, sparks appeared shortly after the

powder is turned on, even if with an enough time of cooling was applied to nanoparticles inside glass reactor.

FTIR technique did not work on finding the oleic acid on ball-milled $SmCo_5$ nanoflakes. The reason is that SmCo5 nanopartiles are thousands time larger than $CoFe_2O_4$ nanoparticles, and because of high ratio of surface area for these particles much more oleic acid left on cobalt ferrite nanoparticle surface. The amount of oleic acid on $SmCo_5$ nanoparticles is too scarce to be detected by FTIR. XRD results of plasma treated $SmCo_5$ nanoparticles showed that Cobalt (FCC) peak started to appear in case of long time treatment. This is probably due to the sparks occurrence when the treating time is long enough, typically over 60 minutes, which the local temperature of the sparks was very high so that $SmCo_5$ nanoflakes were partly decomposed. Some XPS results were not agree with expected and the possible explanation is that the agglomeration happened in the nanoparticles during the plasma treatment, which yielded an inhomogeneous plasma treatment and big difference between different XPS results. Further work is highly needed to clarify these behaviors.

References

1. Narayan Poudyal, Master Thesis, the University of Texas at Arlington, 2005.
2. Soshin Chikasumi, “Physics of Magnetism” John Wiley and Sons, (1964).
3. B.D.Cullity, “Introduction to Magnetic Materials”, Addison-Wesley Publishing, (1972).
4. Nicola A. Spaldn, “ Magnetic Materials: Fundamentals and Device Applications”, Cambridge University Press, (2003).
5. William D. Callister, Jr., “Material Science and Engineering: An Introduction”, John Wiley & Sons, 2000.
6. Robert C. O’ Handley, “Modern Magnetic Materials: Principles and Applications”, Wiley & Sons, 2000.
7. http://www.azom.com/details.asp?ArticleID=637.
8. C. A. Crouse, E. Michel, Y. Shen, S. J. Knutson, B. K. Hardenstein et al, “Effect of surfactant molecular weight on particles morphology of $smCo_5$ prepared by high energy ball milling”,*Journal of Applied Physics*, 111, 07A724(2012).
9. Narayan Poudyal and J Ping Liu, “Advances in nanostructured permanent magnets research”, *J. Phys. D: Appl. Phys*, 46, 043001(2013).
10. Liyun Zheng, Alexander M. Gabay, Wanfeng Li, Baozhi Cui, and George C. Hadjipanayis, “Influence of the type of surfactant and hot compaction on the magnetic properties of $SmCo_5$ nanoflakes”, *JOURNAL OF APPLIED PHYSICS*,109,07A721(2011).
11. Alfred Grill, “Cold Plasma in Materials Fabrication: FROM FUNDAMENTALS TO APPLICATIONS”, IEEE PRESS, 1993.
12. N.T. Rosell, Ph.D. Thesis, Ramon Llull University, Barcelona, 2008.
13. BMBF, German Federal Ministry of Education and *Research* “*Plasma Technology: Process Diversity and Sustainability”*, Bonn 2001.

14. I. Hudec and M. Jaso, Influence of plasma polymerizationon Adhesion of Polyester Cords to Rubber Matrix, presented at the KHK, Hannover, Germany November 2006.
15. F.Bretagnol, M.Tatoulian, F.Arefi-Khonsari, G. Lorang, J. Amouroux, Surface Modification of polyethylene powder by nitrogen and ammonia low pressure plasma in a fluidized bed reactor. Reactive & Functional Polymers 61 (2004) 221.
16. D. Pappas, A. Bujanda, J. D. Demaree, J. K. Hirvonen, W. Kosik, R.Jensen and S.McKnight, Surface modification of polyamide fibers and films using atmospheric Plasmas, Surface and Coatings Technology, 20 (2006) 4384.
17. D. P. Norton and S. Pearton, Dry Etching of Electronic Oxides, Polymers, and Semiconductors, Plasma Process Polym. 2 (2005) 1.
18. H.Yasuda, Plasma Polymerization, Academic Press London (1985).
19. A. A. Meyer-Plath, K. Schröder, B. Finke and A. Ohl, Current trends in biomaterial surface functionalization—nitrogen-containing plasma assisted processes with enhanced selectivity 7 (2003) 391.
20. B.Gupta, J.Hilborn Ch. Hollenstein, C.J.G.Plummer,; R.Houriet, N. Xanthopoulos, Surface modification of polyester films by RF plasma. Journal of Applied Polymer Science 78 (2000) 108.
21. Campbell S J, Kaczmarek W A, Wu E and Jayasunya K D 1994 *IEEE Trans. Magn.* 30 742.
22. Kaczmarek W A and Ninham B M 1995 *Mater. Chem. Phys.*40 21.
23. Kirkpatrick E M, Majetich S A and McHenry M E 1996 *IEEE Trans. Magn.* 32 4502.
24. Yunhua Wang, Lu Zhou, Baoshan Jia, Duanyuan Bai, Xu Yang, Xin Gao, Baoxue Bo, “The Effect of Argon Plasma Cleaning on the Surface Characteristic of GaAs Substrate”, 2012 International Conference on Optoelectronics and Microelectronics (ICOM).

25. D. F. O'Kane and K. L. Mittal, “Plasma cleaning of metal surfaces”, *J. Vac. Sci. Technol*. 11, 567 (1974).
26. C. Martınez, S. Kyrsta, R. Cremer and D. Neuschutz, “Application of argon r.f. plasma etching for the removal of oxidic scales on ULC steels”, *Surf. Interface Anal.* 2002; 34: 396–399.
27. www.nordson.com/en-us/divisions/march/support/Literature/Documents/2-argonplasma.pdf
28. A.Belkind and S.Gershman, “Plasma Cleaning of Surfaces”, Vacuum Technology & Coating 2008.
29. Yiping Wang, Yang Li, Chuanbing Rong and J Ping Liu, “Sm–Co hard magnetic nanoparticles prepared by surfactant-assisted ball milling”, Nanotechnology 18 (2007) 465701 (4pp).
30. Jing Wu, Master Thesis, the University of Texas at Arlington, 2005.
31. Sulak Sumitsawan, Ph. D. Thesis, the University of Texas at Arlington, 2011.
32. http://en.wikipedia.org/wiki/Oleic_acid.
33. http://en.wikipedia.org/wiki/Carboxylate.
34. Cho, J. H. (2005). “RF pulsed plasma surface modification of titanium dioxide nanoparticles for environmental applications.” Ph. D. Dissertation, the University of Texas at Arlington.

Biographical Information

Mr. Ke Wang earned his bachelor degree in Engineering from China University of Mining and Technology (Beijing) in 2011. In 2011 Spring semester, he was a visiting undergraduate student in Electrical Engineering Department at Pennsylvania State University, working with Dr. Sven Bilen in the field of plasma source verification. It is at Penn State that he started to work on the research field of plasma and developed his research interests in this field. He went to the University of Texas of Arlington in 2011 fall, and he kept working on plasma under the supervision of Dr. J.Ping Liu and Dr. Richard Timmons. After he gets his master degree at the University of Texas at Arlington, he will go to Ryerson University to pursue his PhD degree in Mechanical and Industrial Engineering and start his new career at Toronto, Canada.